Supporting Information

Carbon and chlorine isotope fractionation patterns associated with different engineered chloroform transformation reactions

Clara Torrentó[†‡*], Jordi Palau[†‡], Diana Rodríguez-Fernández[‡], Benjamin Heckel[§], Armin Meyer[§], Cristina Domènech[‡], Mònica Rosell[‡], Albert Soler[‡], Martin Elsner[§], Daniel Hunkeler[†]

†Centre for Hydrogeology and Geothermics, Université de Neuchâtel, 2000 Neuchâtel, Switzerland.

‡Grup de Mineralogia Aplicada i Geoquímica de Fluids, Departament de Mineralogia, Petrologia i Geologia Aplicada, Facultat de Ciències de la Terra, Martí Franques s/n, Universitat de Barcelona (UB), 08028 Barcelona, Spain.

§Institute of Groundwater Ecology, Helmholtz Zentrum München, 85764 Neuherberg, Germany.

Corresponding Author:

*Clara Torrentó Phone: +41 32 718 26 49; Fax: +41 32 718 26 03, e-mail: clara.torrento@unine.ch

Total number of pages (including cover): 25

Figures: 4

Tables: 2

CHEMICALS

Dibasic anhydrous sodium phosphate (Na_2HPO_4, Panreac AppliChem, Barcelona, Spain) and sodium hydroxide (NaOH, Baker, Phillipsburg, NJ, USA) were used to prepare a solution buffered at pH 12 consisting of 0.05 M Na_2HPO_4 and 0.1 M NaOH. A pH 7 phosphate-buffer solution was prepared from 0.2 M potassium dihydrogen phosphate (KH_2PO_4, Merck kGaA, Darmstadt, Germany) and 0.2 M Na_2HPO_4 solutions. Sodium peroxodisulfate ($Na_2S_2O_8$, Sigma-Aldrich, St Louis, MO, USA) solutions of different concentrations (i.e. 88, 176 and 704 mM) were prepared less than three hours before starting the experiments. A 1 M acetic acid solution was prepared from glacial acetic acid (CH_3CO_2H, Sigma-Aldrich). A 0.2 mM HEPES (99.5%, Sigma-Aldrich) pH 6.6 buffer solution was also prepared.

A saturated CF solution was prepared by adding pure chloroform (99%, Sigma-Aldrich) to distilled water in a concentration exceeding its solubility at room temperature and stirring upside down overnight in amber glass bottles without headspace. An aqueous CF stock solution containing 2100 mg L^{-1} was prepared from the saturated solution and preserved at 4 °C until use. For the experiments with Fe(0), pure CF (99%, Alfa Aesar, Ward Hill, MA, USA) was used.

The cast iron (92% purity) was obtained from Gotthart Maier Metallpulver GmbH (Rheinfelden, Germany). To reduce the oxidized coating on the iron surface, prior to the experiments the iron was acid-cleaned and dried under anoxic conditions inside a chamber containing a gas mixture of 90% N_2 and 10% H_2. During acid cleaning, the Fe was soaked in degassed 1 M hydrochloric acid solution (HCl, 32 wt. %, Sigma-Aldrich) for 1 h, then rinsed five times with degassed deionized water, and dried overnight (Matheson and Tratnyek, 1994; Dayan et al., 1999; Slater et al., 2002). The iron was weighed before and after the treatment to verify its dryness. The specific surface area was measured by N_2 gas adsorption (Brunauer-Emmett-Teller, BET method) (Brunauer et al., 1938) before (1.00±0.01 m^2g^{-1}) and after (1.624±0.007 m^2g^{-1}) the acid cleaning indicating that this procedure increased the potential reactive surface. The particle size distribution of the iron particles was determined using a particle size analyzer (Beckman Coulter, Inc., Fullerton, CA, USA) and by photon correlation spectroscopy (Beckman Coulter, model N5) as between 0.4 to 2.0 mm, where the average diameter was 1.2 mm. Hence it is considered to be milli-sized ZVI and, therefore, compared to micro-sized rather than to nano-sized iron throughout the paper.

ANALYTICAL METHODS

Chemical analyses

Concentration measurements of chlorinated compounds were performed by headspace (HS) using GC/MS or GC/TOF/MS. The GC/MS system, located in the Scientific and Technological Centers of the University of Barcelona (CCiTUB), consisted of a FOCUS Gas Chromatograph (GC) coupled with a DSQ II Mass Spectrometer (MS, Thermo Fisher Scientific, Waltham, MA, USA). Compounds were separated in a DB-624 column (60 m × 0.32 mm × 1.8 µm, Agilent, Palo Alto, CA, USA) with helium as the carrier gas (flow of 1.8 mL min^{-1}). The column was initially held at 60 °C for 2 min, ramped at 8 °C min^{-1} to 220°C and held at 220 °C for 5 min. The HS procedure was conducted for 30 min at 80 °C in 20 mL headspace vials containing 15 mL of sample. For the experiments of CF oxidation by PS, the agitation was performed at room temperature in order to avoid heat-activation of PS and CF degradation in the agitator unit. A headspace volume of 0.75 mL was injected in split mode (22:1 split ratio) at 220 °C through a split/splitless injector using a Triplus headspace autosampler (Thermo Fisher Scientific). The interface and the ionization source were set to 260 °C and 200 °C, respectively and MS (EI, 70 eV) was performed in full scan mode between 35 and 350 amu. Concentration calculations were performed using seven point calibration curves. The error based on replicate measurements was around 5% for all the compounds. For the experiments with Fe(0), a GC/TOF/MS system from the Institute of Groundwater Ecology of the Helmholtz Zentrum München was used, which consisted of a Dani Master 10115004 GC coupled to a time-of-flight (TOF) and an Agilent 5975C MS. Compounds were separated in a VOCOL column (30 m × 0.25 mm × 1.5 µm, Supelco) with helium as the carrier gas (flow 1.4 mL min^{-1}). The column was initially held at 60 °C for 2 min, ramped at 8 °C min^{-1} to 165°C, then ramped at 25 °C min^{-1} to 220°C and finally held at 220 °C for 1 min. The HS procedure was conducted for 5 min at 40 °C in 10 mL headspace vials containing 1 mL of sample. A headspace volume of 1 mL was injected in split mode (10:1 split ratio) at 250 °C through a split/splitless injector using a Combi Pal autosampler (CTC Analytics). Concentration calculations were performed using seven point calibration curves. The error based on replicate measurements was around 5% for all the compounds. In addition, chloride anions concentrations were analyzed by high-performance liquid chromatography (HPLC) using a WATERS 515 HPLC pump with IC-PAC Anion column and WATERS mod 432 detector and pH evolution was monitored using a Labor-pH-Meter Lab 850 Messparameter (SI-Analytics GmbH, Mainz, Germany).

Stable Isotope Ratio Measurements

Carbon isotope analyses of CF and some detectable volatile daughter products were performed using two different GC/IRMS systems. The GC/IRMS-1, located in the University of Neuchâtel, consisted of a 7890A GC (Agilent, Santa Clara, CA, USA) coupled to an Isoprime™ 100 isotope ratio mass spectrometer (IRMS) via an Isoprime™ GC5 combustion interface set to 970 °C (Isoprime Ltd., Manchester, UK). Aqueous samples and standards were prepared in 42-mL VOC vials without headspace and preconcentrated with a Stratum purge & trap system (Teledyne Tekmar Dohrmann, Mason, OH, US) connected to a cryogenic trap (Teledyne Tekmar Dohrmann). A 25 mL sample volume was purged with N_2 at 40 mL min^{-1} for 10 min and the degassed compounds were retained on a VOCARB 3000 trap (Supelco, Bellefonte, PA, US) at room temperature. After desorption from the trap at 250 °C, the compounds were condensed in the cryogenic unit at -80 °C, released by heating to 180 °C and injected by splitless mode into the GC. The GC was equipped with a DB-VRX column (60m x 0.32 mm x 1.8 µm) (Agilent, Santa Clara, CA, US). Helium was used as carrier gas at 1.7 mL min^{-1} and the oven temperature was initially held at 40°C for 6 min, increased to 130 °C at 10 °C min^{-1} (0.1 min)

and increased to 220°C at 20°C min^{-1} and held for 1 min at 220°C. Aqueous samples and isotopic standards interspersed along the sequence were diluted to a similar concentration and one of every three samples was analyzed twice as a quality control. The analytical uncertainty 2σ of carbon isotopic measurements with the GC/IRMS-1 was ±0.3‰ obtained from a total of 11 standard injections along the analyzing period.

For the experiments with Fe(0), the GC/IRMS-2 available in the CCiTUB was used as described elsewhere (Torrentó et al., 2014). The system consisted of a Thermo Finnigan Trace GC Ultra instrument coupled via a GC-Isolink interface to a Delta V Advantage IRMS (Thermo Scientific GmbH, Bremen, Germany). This GC was equipped with a Supelco SPB-624 column (60 m × 0.32 mm × 1.8 µm, Bellefonte, PA, USA). The oven temperature program was kept at 60 °C for 5 min, heated to 165 °C at a rate of 8 °C min^{-1}, heated to 220 °C at 25 °C min^{-1} and finally held at 220 °C for 1 min. The injector was set to split mode with a split ratio of 1:5 at a temperature of 250 °C. Helium was used as a carrier gas (2.2 mL min^{-1}). The VOCs were extracted from the aqueous samples by automated headspace solid-phase micro-extraction (HS-SPME) using a 75-µm Carboxen-PDMS fiber (Supelco, Bellefonte, PA, USA). The 20-mL vials filled with 10-mL aqueous samples were placed in a TriPlusTM Autosampler equipped with a SPME holder (Thermo Fisher Scientific, Waltham, USA). Samples were extracted for 20 minutes at 40 °C and constant agitation (600 rpm) and the SPME fibers were desorbed for 5 min at 250 °C. To correct slight carbon isotopic fractionation induced by the HS-SPME preconcentration technique (Palau et al., 2007), the samples delta values obtained with the GC/IMRS-2 were corrected by daily values of calibrated in-house standards of known C isotope ratios, prepared at the same concentration range than the samples and that were previously determined using a Flash EA1112 (Carlo-Erba, Milano, Italy) elemental analyzer (EA) coupled to a Delta C isotope ratio mass spectrometer (Thermo Fisher Scientific, Bremen, Germany) through a Conflo III interface (Thermo Finnigan, Bremen, Germany) using four international reference materials (USGS 40, IAEA 600, IAEA CH6, IAEA CH7) with respect to the Vienna Pee Dee Belemnite (VPDB) standard, according to Coplen et al. (2006). The analytical uncertainty 2σ of carbon isotopic measurements with the GC/IRMS-2 was ±0.5‰ obtained from a total of 16 standard injections along the analyzing period.

Chlorine isotope CF analyses were performed using a GC/qMS system from the University of Neuchâtel or a GC/IRMS system from the Institute of Groundwater Ecology of the Helmholtz Zentrum München (GC/IRMS-3). An interlaboratory comparison of the two analytical methods can be found in Heckel et al. (2017). The GC/qMS system consisted of a 7890A GC coupled to a 5975C qMS (Agilent, Santa Clara, CA, US). Samples were prepared in 20-mL HS vials filled with 15 mL of solution. After incubating at 60 °C for 2 min, headspace samples of 1 mL were injected in the split/splitless injector (1:20 split ratio) at 250 °C using a CombiPal autosampler (CTC Analytics, Zwingen, Switzerland). For the experiment of CF oxidation by PS, the extraction was performed at room temperature in order to avoid heat-activation of PS and CF degradation in the agitator unit. The GC was equipped with a DB-5 column (30 m x 0.25 mm x 0.25 µm, Agilent, Santa Clara, CA, US). The He flow rate was 1.2 mL min^{-1} and the temperature program was 70 °C (2 min), followed by a ramp of 20 °C min^{-1} to 230 °C. A dwell time of 50 msec was defined for all measurements and positive electron impact ionization at 70 eV was used.

For chlorine isotope CF analyses of the samples for the Fe(0) experiment, the GC/IRMS-3, located in the Institute of Groundwater Ecology of the Helmholtz Zentrum München, was used. It consisted of a Trace GC coupled to a MAT 253 IRMS with dual inlet system via a heated transfer line. The GC was equipped with a VOCOL column (30 m × 0.25 mm × 1.5 µm, Supelco) with Helium as the carrier gas

(flow 1.4 mL min^{-1}). The column was initially held at 60 °C for 2 min, ramped at 8 °C min^{-1} to 165 °C, then ramped again at 25 °C min^{-1} to 220°C and finally held at 220 °C for 1 min. The HS procedure was conducted for 5 min at 40 °C in 10 mL headspace vials containing 1 mL of sample. A headspace volume of 1 mL was injected in split mode (1:10 split ratio) at 220 °C through a split/splitless injector.

For the GC/qMS, average $\delta^{37}Cl$ values were determined on the basis of ten injections of each sample while two external working standards were interspersed along the sequence. Raw values were determined by referencing versus one of the external working standard according to Eq. 1. Precision 2σ of chlorine isotopic measurements using this system was in all the cases below ±0.5‰ based on replicate measurements. In the GC/IRMS-3, six measurements of the external working standards were performed at the beginning, two during and four at the end of each sequence. Pure CF was used as monitored gas and three reference gas peaks were run at the beginning and at the end of each analysis run. Raw $\delta^{37}Cl$ values were determined by automatic evaluation of selected CF ion peaks against the reference gas peaks. The analytical uncertainty 2σ of chlorine isotopic measurements using the GC/IRMS-3 was ±0.2‰. The peak intensities of the two most abundant fragment ions (m/z 83 and 85) were measured by GC/qMS whereas two fragment ions (m/z 47 and 49) were used for the GC/IRMS-3 measurements. These ion couples correspond to the isotopologue pairs ($[^{35}Cl_2{}^{12}C^1H]^+$ and $[^{35}Cl^{37}Cl^{12}C^1H]^+$) and ($[^{35}Cl^{12}C]^+$ and $[^{37}Cl^{12}C]^+$), respectively. The isotope ratio was obtained from the ratio of these isotopologues according to Eq. SI2 (Elsner and Hunkeler, 2008).

$$R = \frac{^{37}Cl}{^{35}Cl} = \frac{^{37}p}{^{35}p} = \frac{k}{(n-k+1)} \cdot \frac{^{37}Cl_{(k)}{}^{35}Cl_{(n-k)}}{^{37}Cl_{(k-1)}{}^{35}Cl_{(n-k+1)}} = \frac{1}{2} \cdot \frac{^{85}I}{^{83}I} = \frac{^{49}I}{^{47}I} \quad \text{(SI2)}$$

where ^{37}p and ^{35}p are the probabilities of encountering ^{37}Cl and ^{35}Cl, n is the number of Cl atoms, k is the number of ^{37}Cl isotopes, $^{37}Cl(k)$ $^{35}Cl(n-k)$ and $^{37}Cl(k-1)$ $^{35}Cl(n-k+1)$ represent the isotopologues containing k and (k−1) heavy isotopes, respectively, and I indicates the ion peak intensities. In both cases, the conversion to delta values relative to the SMOC was performed by an external two-point calibration analyzing two external working standards according to Bernstein et al (2011) (CF-F, 99.5% Fluka; CF-A, 99% Alfa Aesar), with $\delta^{37}Cl_{SMOC}$ values of -3.0±0.2‰ (n=17) and -5.4±0.3‰ (n=8), respectively. The isotope composition of these standards was determined in Waterloo (Isotope Tracer Technologies Inc., Waterloo, Canada) by IRMS after conversion of CF to CH_3Cl using the method developed by Holt et al. (1997).

KINETICS

Data for aqueous concentrations of CF versus time were fit to a pseudo-first-order rate model:

$$dC/dt = - k' C \quad \text{(SI3)}$$

where C is the chlorinated target compound concentration, t is time and k' is the pseudo-first-order rate constant. The k' was obtained using the integrated form of Eq. SI3:

$$\ln C = \ln C_0 - k' t \quad \text{(SI4)}$$

where C_0 is the initial concentration of the chlorinated compound. Uncertainty was obtained from 95% confidence intervals (CI).

For CF reductive dechlorination with Fe(0), a surface-area-normalized reaction rate constant (k_{SA}) was calculated for comparison with other studies. Dechlorination can be described by Eq. SI5 (Matheson and Tratnyek, 1994; Johnson et al., 1996):

$$dC/dt = - k' C = -k_{SA}\, a_S\, \rho_m\, C \quad \text{(SI5)}$$

where α_S is the specific surface area of metal and ρ_m is the mass concentration of Fe(0).

PS oxidation. This reaction followed pseudo-first-order kinetics with a k' of 0.40±0.06 d^{-1} (R^2= 0.96, Fig S1). Kinetics of the experiments with initial molar ratios of 10/1 and 5/1 are shown in Fig S2. Kinetics of CF oxidation by thermally-activated PS were not described so far as Huang et al. (2005) found no degradation of CF after 72 h reaction with 5 g L^{-1} of sodium PS activated at 40°C in a mixture of 59 VOCs. Our k' is similar to the values (0.1 and 0.2 d^{-1}) reported by Zhu et al. (2015) for CF oxidation with PS activated by Fe(II) at a PS/CF molar ratio much higher (12400/1). Reaction with UV-activated PS at a PS/CF molar ratio of 290/1 resulted in higher k' values (between 30 and 300 d^{-1}, Jung et al., 2015).

Alkaline hydrolysis. The reaction followed pseudo first order kinetics (R^2= 0.92, Fig S1) with a k' of 0.052±0.008 d^{-1}, which is in agreement with a previously reported rate constant of 0.047±0.004 d^{-1} obtained at a similar pH 11.9±0.1 (Torrentó et al., 2014).

Fe(0) dechlorination. The obtained k' was 0.07±0.01 h^{-1} (R^2= 0.93, Fig S1), which corresponds to a k_{SA} of 2.1±0.4x10^{-2} L m^{-2} d^{-1}. Milli-sized Fe(0) particles were used in the present experiments. The normalized CF degradation rate constant (k_{SA}) obtained here is within a comparable range of values reported previously for CF reductive dechlorination at pH 5-8 with micro-sized iron (between 0.8 and 12.5 x10^{-2} L m^{-2} d^{-1}) (Johnson et al., 1996; Feng and Lim, 2005; Song and Carraway, 2006; Lee et al., 2015) and with nano-sized iron (between 1.2 and 125 x10^{-2} L m^{-2} d^{-1}) (Choe et al., 2001; Feng and Lim, 2005; Song and Carraway, 2006). Mass-transfer control is assumed as limitation affecting the rate constant, according to Arnold et al. (1999). Significant variations among k_{SA} data for a given compound, with over an order of magnitude differences, have been already reported and attributed to variability of the specific surface area (α) of Fe(0) due to iron treatment, differences in grain size distribution and the differences between physical surface area and reactive real surface area (Johnson et al., 1996). The effect of mixing speed on reaction rate constant have been studied to demonstrate the possibility of mass transfer limitations in batch systems for zero-valent iron

reactions, exhibiting a linear relationship of rate constant with respect to $(rpm)^{0.5}$(Agrawal and Tratnyek, 1996). Even though the $(rpm)^{0.5}$ of the present study (14.2) is higher than in some of the referred experiments (4.5-11), the decrease of thickness of concentration boundary layers (increasing fluid velocity relative to the particles) with higher mixing speed is achieved up to a point (Arnold et al., 1999). In spite of the hypothetical lack of control of mixing speed on observed reaction rate, the rate limiting step also may represent either mass transfer to the surface or reaction at the surface (Arnold et al., 1999). External (geometric) surface area of the particles is preferred by some studies rather than the measured BET surface area and the comparison of k_{obs} to surface-area normalized mass transfer coefficients ($k_L a$) as a diagnostic for mass transfer control is recommended (Arnold et al., 1999). Moreover, used cast iron had a prismatic habitus and there is an uncertainty in $k_L a$ associated with particle sphericity and roughness (Roberts et al., 1985). To sum up, mass-transfer control is assumed as limitation affecting the rate constant, according to Arnold et al. (1999), and therefore exhaustive comparison of the obtained k_{SA} with the published values is not performed.

Two degradation pathways have been proposed for CF dechlorination by Fe(0): a reductive elimination pathway to form methane (CH_4) as final product and hydrogenolysis to form dichloromethane (DCM, CH_2Cl_2). CF reduction by micro-sized iron has been reported to occur predominantly via hydrogenolysis producing DCM as the final product (Matheson and Tratnyek, 1994; Feng and Lim, 2005; Song and Carraway, 2006), although the combination of both hydrogenolysis and the elimination pathway to methane has also been shown in studies with micro-sized iron (Feng and Lim, 2005; Li and Farrell, 2000; Támara and Butler, 2004; Lee et al., 2015). In the case of CF reduction with nano-sized iron, the elimination pathway has been reported as the dominant one, yielding to preferential production of methane over DCM (Choe et al., 2001; Feng and Lim, 2005; Song and Carraway, 2006). Lien and Zhang (1999) reported, however, preferential production of DCM with nano-sized iron.

In the present experiments, the yield of DCM, defined as the moles of product formed per mole of CF transformed ($DCM_t/(CF_0 - CF_t)$), where subscripts *0* and *t* indicate initial time and different sampling times, respectively) ranged from 0 to 2.4% over time, showing that accumulation of DCM accounted for only a small part of the initial CF. Similarly, low DCM yields have been previously reported (Choe et al., 2001; Feng and Lim, 2005; Nurmi et al., 2005; Song and Carraway, 2006; Lee et al., 2015). Lee et al. (2015) observed approximately 10% yield of DCM, whereas methane and formic acid accounted for approximately 12% and 5% of the lost CF, respectively, giving a low carbon mass balance of 29%. In the present experiments, analysis of other potential intermediate or end products, such as formic acid, methane or other hydrocarbons, were not performed and mass balance calculations are therefore difficult. Low Cl mass recovery was also observed: after 51 h of experiment, 88% of CF was not anymore in solution, but free chloride and DCM-chlorine only accounted for 35% and 2% of the initial CF-chlorine, respectively. Low mass recoveries during dechlorination of chlorinated ethenes and methanes have been attributed to adsorption of the parent compounds to nonreactive sites of the iron surface (Burris et al., 1995, 1998; Song and Carraway, 2006) or to adsorption of a substantial proportion of produced hydrocarbons intermediates (Hardy and Gillham, 1996; Lee et al., 2015). Compounds in the sorbed phase were in the present experiments not subject to exhaustive extraction for analysis and quantification.

FIGURE S1

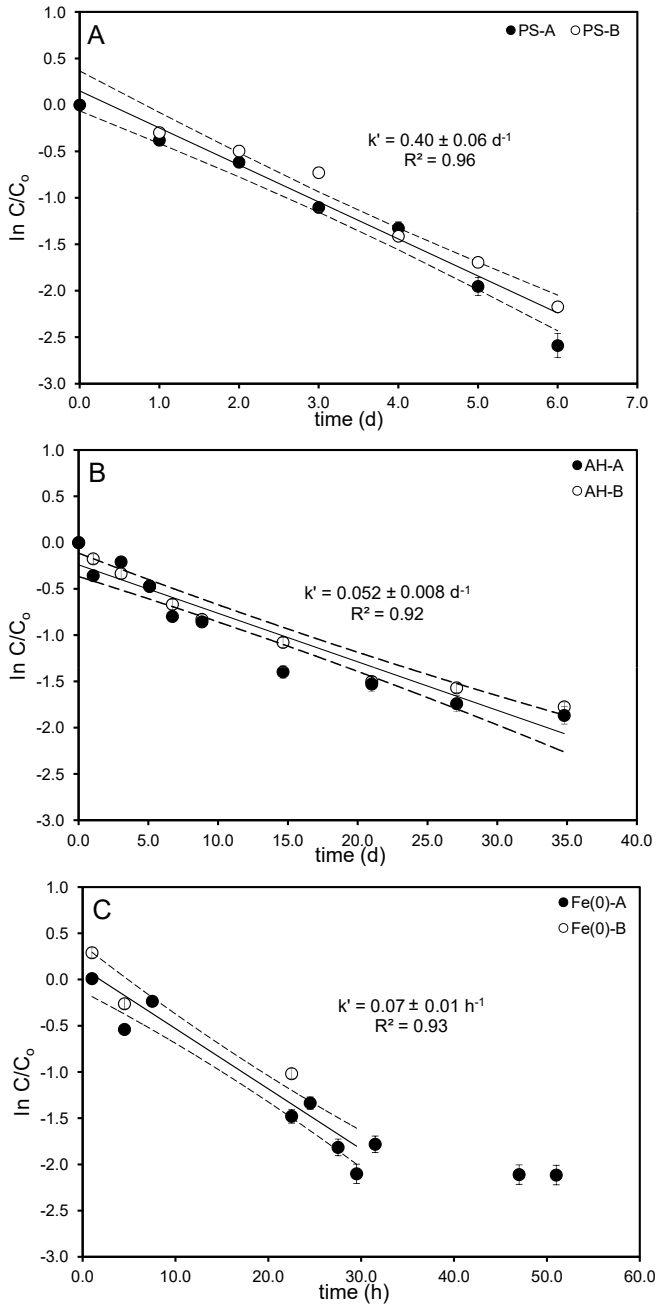

Figure S1. Semi-logarithmic plot of kinetics of CF degradation by oxidation by thermally-activated PS (A), alkaline hydrolysis (B) and dechlorination by Fe(0) (C). Data from the duplicated experiments are shown (i.e. filled and empty symbols). The error bars show the uncertainty in the natural logarithm of C/C_o, calculated by error propagation including uncertainty in concentration measurements. Note that in some cases error bars are smaller than the marker size. Pseudo-first-order rate constants (k') were extracted from curve fittings according to Eq. SI4. Dotted lines represent 95% CI of linear regression. For CF dechlorination with Fe(0), pseudo-first-order rate constant was calculated omitting data after 30 days, after when the disappearance of CF almost stopped.

FIGURE S2

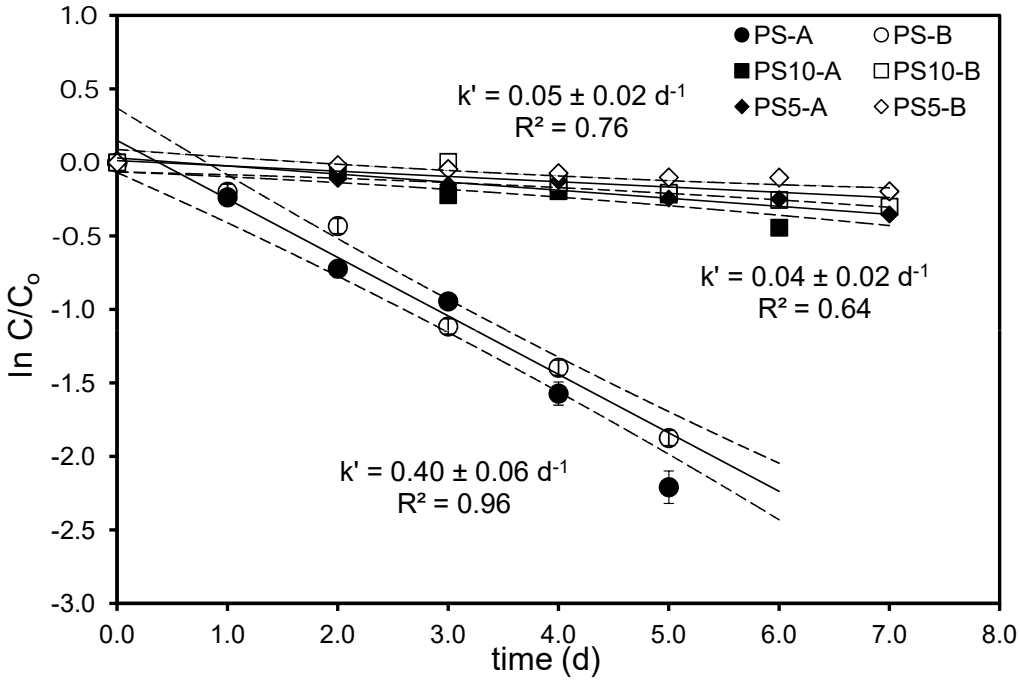

Figure S2. Semi-logarithmic plot of kinetics of CF oxidation with thermally-activated PS with initial PS to CF molar ratios of 5/1 (PS5), 10/1 (PS10) and 40/1 (PS). Data from duplicate experiments (A and B) are shown. Dotted lines represent 95% CI of linear regressions. The uncertainty in the natural logarithm of C/C_o was calculated by error propagation using uncertainty in concentration measurements. In some cases, error bars are smaller than the symbols.

CALCULATION OF APPARENT KINETIC ISOTOPE EFFECTS (AKIE)

Carbon and chlorine AKIE values were calculated by Eq. SI6 (Elsner et al., 2005)

$$\mathrm{AKIE} = \frac{1}{1+\left(\frac{z\,n}{x}\varepsilon_{bulk}\right)} \qquad \text{(SI6)}$$

where n is the number of atoms of the considered element in the molecule, x is the number of these atoms located at the reactive site/s, z is the number of atoms located at the reactive site/s and being in intramolecular competition. The values for n, x, and z were chosen depending on the considered reaction mechanism (see “Mechanistic considerations” section in the main text and “Further discussion in reaction pathways” below). The uncertainty of the AKIE was estimated by error propagation in Eq. SI6.

PRODUCT CARBON ISOTOPE FRACTIONATION TRENDS

During a transformation reaction, the concentration weighted average C isotope ratio of all products ($\delta^{13}C_{P,\,average}$) can be obtained using an isotope mass-balance equation:

$$\delta^{13}C_{0,S} = f \times \delta^{13}C_S + (1-f) \times \delta^{13}C_{P,\,average} = f \times (\delta^{13}C_{0,S} + \varepsilon \ln f) + (1-f) \times \delta^{13}C_{P,\,average} \quad \text{(SI7)}$$

where $\delta^{13}C_{0,S}$ is the initial isotope ratio of the substrate. Rearrangement of Eq. SI7 leads to:

$$\delta^{13}C_{P,average} = \delta^{13}C_{0,S} - \frac{f \times \varepsilon_C}{1-f} \times \ln f \quad \text{(SI8)}$$

Using the parameter D(δ^{13}C) (D(δ^{13}C)=$\delta^{13}C_P$ - $\delta^{13}C_{P,average}$), which expresses how much a particular product isotope ratio deviates from the weighted average of all products (Elsner et al., 2008), Eq. SI9 can be derived:

$$\delta^{13}C_P = \left(\delta^{13}C_{0,S} + D(\delta^{13}C)\right) - \varepsilon_C \times \frac{f \times \ln f}{(1-f)} \quad \text{(SI9)}$$

where $\delta^{13}C_P$ is the isotope ratio of the product measured during the course of the reaction. As kinetic isotope effects of parallel pathways do not change during a reaction, D(δ^{13}C) also remains constant.

For the experiment with Fe(0), carbon isotope data of the reaction product (DCM) was evaluated using Eq. SI9. The DCM isotope trend was fitted in Sigma Plot according to Eq. SI9 with εC and D(δ^{13}C) as fitting parameters. The error of the parameter D(δ^{13}C) is given as the 95% CI of the regression.

The following fit equation was used in Sigma Plot.

$f = a - ((k) \times (x \times \ln(x))/(1 - x))$

where f is fitted to the dependent variable ($\delta^{13}C_{DCM}$), the independent variable x corresponds to f (i.e. C/C_0), a is the coefficient from which D(δ^{13}C) is estimated, and the coefficient k is ε from DCM data. ε from DCM data is identical to ε for CF data, because all carbon isotopes are transferred from reactant to product so that the product isotope curve reflects the enrichment trend of the original atoms in the reactant.

Subsequently, the product-related isotope fractionation $\varepsilon^C_{substrate \rightarrow product}$ was calculated by Eq. SI10:

$$\varepsilon^C_{substrate \rightarrow product} = \delta^{13}C_{0,P} - \delta^{13}C_{0,S} = D(\delta^{13}C) + \varepsilon_C \quad \text{(SI10)}$$

where $\delta^{13}C_{0,P}$ represents the initial isotopic composition of the product. The uncertainty was estimated by error propagation. Eq. SI10 is solely based on isotope measurements of the substrate and a given product and therefore it allows the determination of $\varepsilon^C_{substrate \rightarrow product}$ even without knowledge of absolute reaction rates, product distribution, or closed molar balances (Elsner et al., 2008).

FIGURE S3

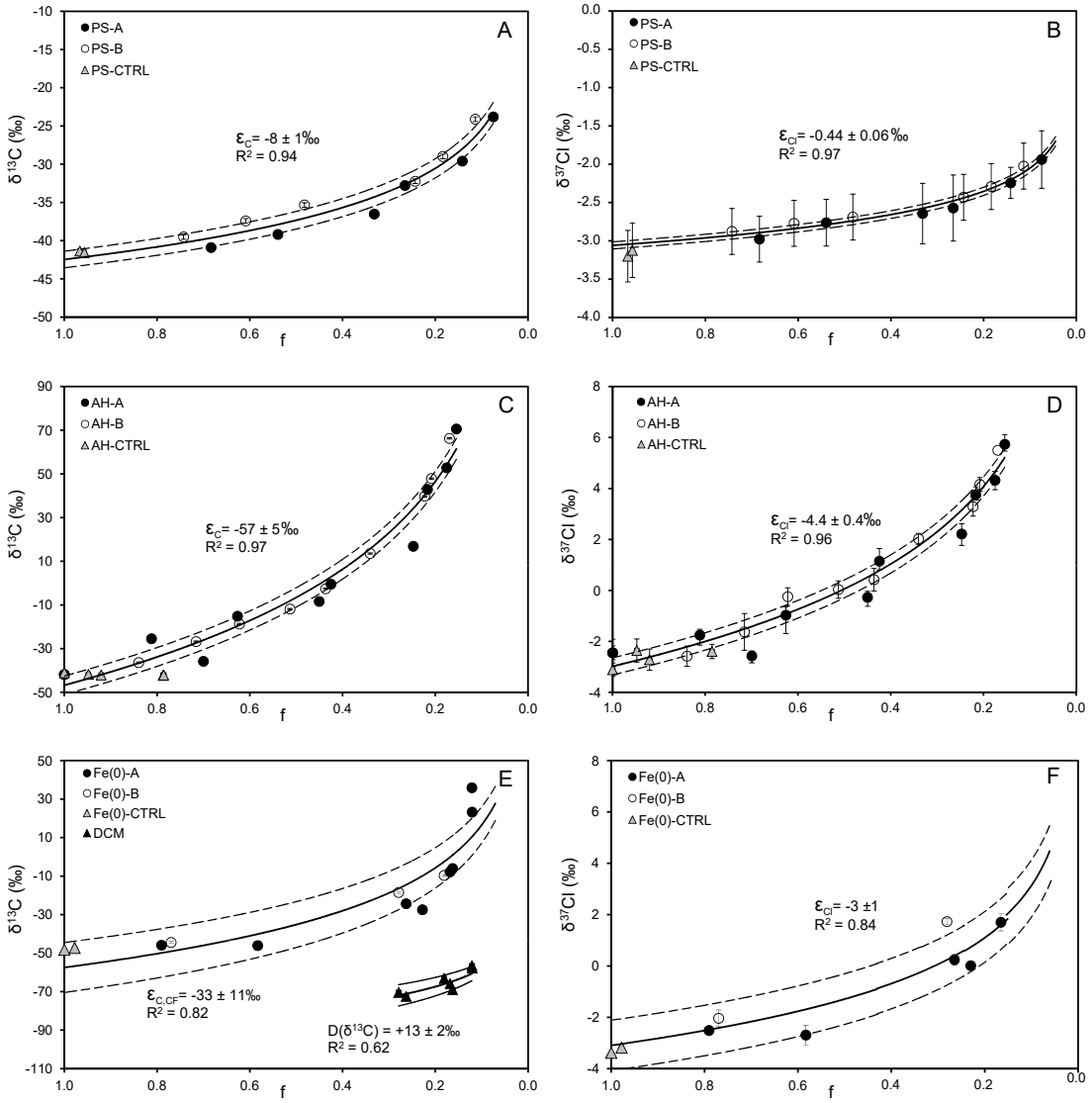

Figure S3. Isotope fractionation patterns in CF of $\delta^{13}C$ (left panels) and $\delta^{37}Cl$ (right panels) measured during oxidation by PS (A and B), degradation by alkaline hydrolysis (C and D) and dechlorination by Fe(0) (E and F). Isotopic fractionation values for both carbon and chlorine were extracted from curve fittings according to the Rayleigh equation (Eq. 1, see Fig 2 in the main text for the Rayleigh plots). Data from the duplicated experiments (i.e. filled and empty symbols) and from the control experiments are shown. Error bars of individual data points indicate standard deviations. For the experiment with Fe(0), the isotope fractionation pattern of DCM is also shown. The dashed curve shows the fit of the DCM isotope data according to Eq. SI9. The uncertainties for given ε are 95% CI.

FURTHER DISCUSSION IN REACTION PATHWAYS

Table S1 shows the obtained AKIE values for different mechanistic scenarios checked for each CF degradation experiment, as well as the comparison with the expected values. See also table S2 for typical C and Cl AKIE values estimated in different studies.

TABLE S1

Table S1. Derived C and Cl AKIE values assuming different reaction scenarios for CF degradation by PS, alkaline hydrolysis (AH) and Fe(0).

	Mechanistic scenario	C parameters	$AKIE_C$	Streitwieser limit KIE_C	typical $AKIE_C$	Cl parameters	$AKIE_{Cl}$	Streitwieser limit KIE_{Cl}	Typical $AKIE_{Cl}$	Scenario consistent
PS	Oxidative C-H bond cleavage	n=x=z=1	1.008 ± 0.001	1.021	1.00 to 1.03	n=x=3 z=1	1.00045± 0.00004	-	small secondary $AKIE_{Cl}$	yes
PS	C-Cl bond cleavage	n=x=z=1	1.008 ± 0.001	1.057	1.01 to 1.03	n=x=z=3	1.00134 ±0.00004	1.013	1.008 to 1.01	no
AH	$E1_{CB}$ elimination	n=x=z=1	1.061 ± 0.006	1.057		n=x=z=3	1.0133 ± 0.0004	1.013		yes
AH	S_N2 substitution	n=x=z=1	1.061 ± 0.006	1.057	1.03 to 1.09	n=x=z=3	1.0133 ± 0.0004	1.013	1.006 to 1.009	yes
Fe(0)	C-Cl bond cleavage	n=x=z=1	1.034 ± 0.012	1.057	1.027-1.033	n=x=z=3	1.008 ± 0.001	1.013		yes

PS oxidation. Initial C-H bond cleavage is the most plausible mechanistic scenario but initial C-Cl bond cleavage scenario was also checked. A primary KIE_{Cl} is only expected for the latter case, where x = z = 3 as the three C-Cl bonds are equivalent and compete for reaction. In the oxidative C-H bond cleavage scenario only a secondary KIE_C occurs. Thus, the following parameters for calculation of $AKIE_{Cl}$ have to be used: x = 3 and z = 1 since any of the three C-Cl bond is broken, and there is, therefore, no intramolecular competition between the three Cl atoms. The obtained C and Cl AKIEs are only consistent with an oxidative C-H bond cleavage mechanism. Therefore, it is proposed a reaction pathway involving the cleavage of the C-H as the rate-limiting step by abstraction of the hydrogen atom from the molecule by the attack of any of the radicals formed after persulfate activation. Although no intermediates were detected, it may be hypothesized that trichloromethanol (Cl_3COH) could form, which would rapidly undergo an elimination reaction to yield phosgene (CCl_2O) (Pohl et al., 1977) that would further hydrolyze to chloride and CO_2 (Pohl et al., 1977). In order to track more confidently the proposed mechanism, hydrogen isotope fractionation during CF oxidation with thermally-activated PS might be further measured.

Alkaline hydrolysis. During alkaline hydrolysis, the rate-limiting step is expected to be the cleavage of the C-Cl bond and thus only one $AKIE_{Cl}$ scenario is possible: x = z = 3 as the three C-Cl bonds are equivalent and compete for reaction. The obtained $AKIE_C$ and $AKIE_{Cl}$ values indicate the involvement of a C-Cl bond in the first rate-limiting step. In principle, the Cl kinetic isotope effect estimated in the present study is, therefore, consistent with the occurrence of a carbanion mechanism but also with a C-Cl bond cleavage via a concerted one-step S_N2 nucleophilic substitution mechanism. There is some

uncertainty in the literature whether a one-step S_N2 nucleophilic substitution mechanism could be a viable option for alkaline hydrolysis of CF in aqueous solution. This mechanism is thermodynamically favorable for gas-phase reaction of OH^- with CF (Borisov et al., 2001). For the reaction in aqueous solution, in contrast, Hine (1950), Valiev et al. (2007) and Kowalski and Valiev (2009) concluded that the S_N2 mechanism is unlikely to play a major role due to the high estimated reaction energy barriers based on experimental and computational chemical data. Since the $E1_{CB}$ mechanism, therefore, seems most plausible for this reaction, further deuterium-exchange experiments might be performed to confirm the existence of a carbanion intermediate as a way to further corroborate the occurrence of the stepwise elimination mechanism (Skell and Hauser, 1945).

Fe(0) dechlorination. The obtained $AKIE_C$ and $AKIE_{Cl}$ values point to cleavage of a C-Cl bond in the first rate-limiting step, which is compatible with the two-step pathway that is commonly hypothesized for this reaction. The first step involves the transfer of a single electron from the metal surface causing the removal of a chlorine atom and the formation of a dichloromethyl radical ($^{\cdot}CHCl_2$), which can undergo two parallel degradation pathways: (1) a reductive elimination pathway to form chloromethyl carbene ($:CHCl$), which can be further reduced to methane (CH_4) as final product, or can be hydrolyzed to give off HCl and carbon monoxide (CO) that can further be converted to formate ($HCOO^-$) and/or methane; (2) hydrogenolysis to form dichloromethane (DCM, CH_2Cl_2), the latter being the dominant pathway for micro-sized iron (Matheson and Tratnyek, 1994; Feng and Lim, 2005; Song and Carraway, 2006). In all the cases, cleavage of a C-Cl bond is expected to be the first rate-limiting step.

FIGURE S4

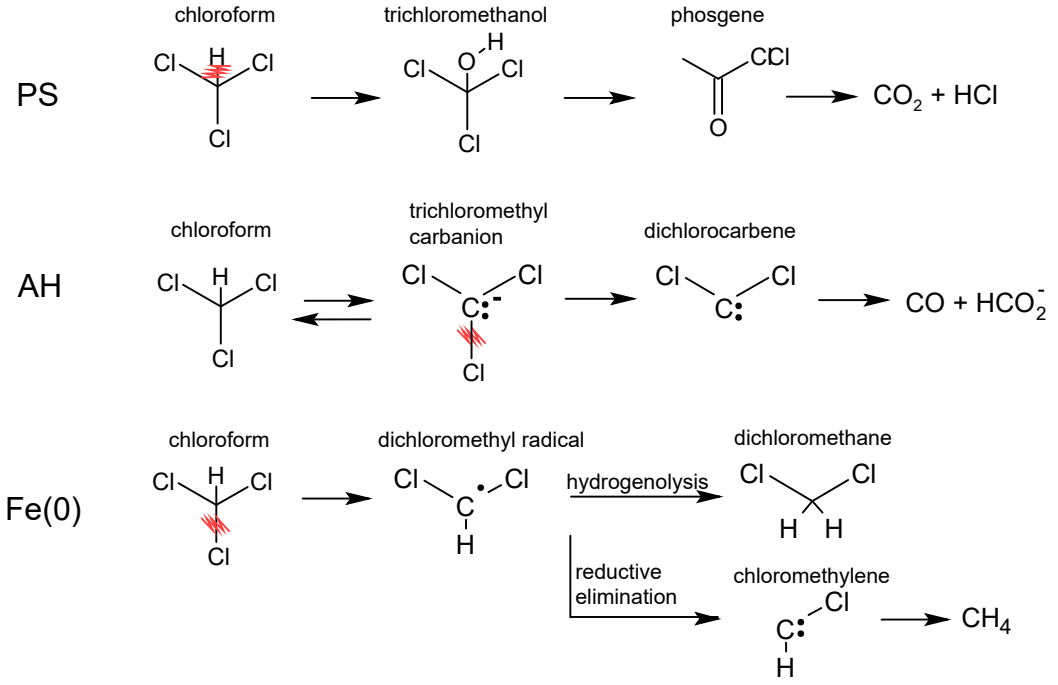

Figure S4. Proposed reaction pathways for chloroform degradation by oxidation with PS (upper scheme), alkaline hydrolysis (middle scheme) and reductive dechlorination with milli-sized Fe(0) (lower scheme).

TABLE S2

Table S2. Comparison of ε and AKIE values for C and Cl isotopes in different studies. Selected examples involving oxidative C-H bond cleavage, the $E1_{CB}$ mechanism, nucleophilic substitution reactions (S_N2-type) and C-Cl bond cleavage are shown.

Compound	Degradation pathway	Type	Conditions	ε_{bulkC} (‰) ± 95%CI	n_C	x_C	z_C	$AKIE_C$	ε_{bulkCl} (‰) ± 95%CI	n_{Cl}	x_{Cl}	z_{Cl}	$AKIE_{Cl}$	$\Lambda \approx \varepsilon C/\varepsilon Cl$	Reference
Oxidative C-H bond cleavage		**Streitwieser limit KIE_C = 1.02 (Elsner et al., 2005)**													
CF	oxidation with thermally-activated PS	abiotic	laboratory	-8 ± 1	1	1	1	1.008 ± 0.001	-0.44 ± 0.06	3	3	1	1.00045± 0.00004[a]	17 ± 2	this study
1,1,1-TCA	oxidation with thermally-activated PS	abiotic	laboratory	-4.0 ± 0.2	2	1	1	1.0081 ± 0.0002	0					∞	Palau et al. (2014a)
1,2-DCA	aerobic oxidation	biotic (*Pseudomonas* sp.)	laboratory	-3.0 ± 0.2	2	2	2	1.006	NM					NM	Hirschorn et al. (2004)
1,2-DCA	aerobic oxidation	biotic (*Pseudomonas* sp. DCA1)	laboratory	-3.5 ± 0.1	2	2	2	1.0070 ± 0.0002	-3.8 ± 0.2	2	2	1	1.0038 ± 0.0002[a]	0.78 ± 0.03	Palau et al. (2014b)
TBNPA	oxidation with H_2O_2/nCuO	abiotic	laboratory	-2.4 ± 0.3	5	4	4	1.012 ± 0.0015	NAP					NAP	Kozell et al. (2015)
Ethylbenzene	oxidation with t-BuOOH	abiotic	laboratory	NA	NA	NA	NA	1.015	NAP					NAP	Merrigan et al. (1999)
Toluene	aerobic oxidation	biotic	laboratory	-0.4 to -3.3	7	5	5	1.000 to 1.030	NAP					NAP	Elsner et al. (2005) ; Vogt et al. (2008)
Toluene	anaerobic oxidation	biotic	laboratory	-0.8 to -6.2	7	1	1	1.006 to 1.044	NAP					NAP	Meckenstock et al. (1999); Vogt et al. (2008); Hermann et al. (2009); Dorer et al. (2016)
MTBE	aerobic oxidation	biotic (Methylibium petroleiphilum PM1)	laboratory	-2.0 to -2.4				1.008-1.012	NAP					NAP	Hunkeler et al. (2001); Gray et al. (2002)
MTBE	aerobic oxidation	biotic (Methylibium sp.)	laboratory	-0.28 to -2.3				1.001-1.011	NAP					NAP	Rosell et al. (2007)
MTBE	aerobic oxidation	biotic (different pure cultures)	laboratory	-1.4 to -2.6				NA	NAP					NAP	Rosell et al. (2010)
MTBE	aerobic oxidation	biotic (US3-M mixed culture)	laboratory	-2.2 to -2.3				1.011	NAP					NAP	Bastida et al. (2010)
atrazine	oxidative N-dealkylation	biotic (*Rhodococcus* NI86/21)	laboratory	-4.0 ± 0.2				1.0040 ± 0.0002	NM					NM	Meyer et al. (2014)
isoproturon	hydroxylation	biotic (Phoma cf. eupyrena Gr61)	laboratory	-1.0 ± 0.2				1.01	NAP					NAP	Penning et al. (2010)
nitrobenzene	dioxygenation	biotic (*Escherichia coli*, purified NBO)	laboratory	-3.5 to -3.7	2	2	2	1.021 to 1.023	NAP					NAP	Pati et al. (2014)

nitrobenzene	dioxygenation	biotic (*Comamonas* JS765)	laboratory	-3.9 ± 0.09	2	2	2	1.024 ± 0.0005	NAP				NAP	Hofstetter et al. (2008)
Stepwise elimination reaction ($E1_{cB}$)		**Streitwieser limit C-Cl bond cleavage KIE_C = 1.057 (Elsner et al., 2005; Aelion et al., 2010)**							**Streitwieser limit C-Cl cleavage KIE_{Cl} = 1.013 (Elsner et al., 2005)**						
CF	Alkaline degradation	abiotic (alkaline hydrolysis)	laboratory	-57 ± 5	1	1	1	1.061 ± 0.006	-4.4 ± 0.4	3	3	3	1.0133 ± 0.0004	13.0 ± 0.8	this study
CF	Alkaline degradation	abiotic (alkaline hydrolysis)	laboratory	-53 ±3	1	1	1	1.056 ± 0.003	NM				NM	Torrentó et al. (2014)
Nucleophilic substitution reactions (S_N2-Type)		**Typical range KIE_C = 1.03 to 1.09 (Elsner et al., 2005)**							**Theoretical range KIE_{Cl} = 1.006 to 1.009 (for CH_3Cl, Dybala-Defratyka et al., 2004)**						
TBNPA	Alkaline degradation	abiotic (alkaline hydrolysis)	laboratory	-10.4 ± 1.6	5	3	3	1.052 ± 0.008	NAP				NAP	Kozell et al. (2015)
DCM	Aerobic oxidation	biotic (MC8b culture)	laboratory	-42.4 ± 1.5	1	1	1	1.044	-3.8 ± 0.3				11,2	Heraty et al. (1999)
CH_3Cl	Aerobic oxidation	biotic (IMB-1, MB-2 and CC495 cultures)	laboratory	-42 to -48	1	1	1	1.044 to 1.050	NM				NM	Miller et al. (2001)
1,2-DCA	Hydrolytic dehalogenation	biotic (*X. autotrophicus* GJ10 and *A. aquaticus* AD20)	laboratory	-29.5 to -32.3	2	2	2	1.060 to 1.068	-4.2 to -4.4	2	2	2	1.0087 ±0.0002	7.7 ±0.2	Hirschorn et al. (2004); Abe et al. (2009); Palau et al. (2014b)
Reductive dechlorination by C–Cl bond cleavage		**Streitwieser limit KIE_C = 1.057 (Elsner et al., 2005; Aelion et al., 2010)**							**Streitwieser limit KIE_{Cl} = 1.013 (Elsner et al., 2005)**						
CF	Reductive dechlorination	abiotic (Fe(0))	laboratory	-33 ± 11	1	1	1	1.034 ± 0.012	-3 ± 1	3	3	3	1.008 ± 0.001	8 ± 2	this study
CF	Reductive dechlorination	abiotic (Fe(0))	laboratory	-30 ± 2	1	1	1	1.03 ± 0.07	NM				NM	Lee et al. (2015)
CF	Reductive dechlorination	biotic (*Dehalobacter* sp. CF50 consortium)	laboratory	-27.5 ± 0.9	1	1	1	1.028± 0.002	NM				NM	Chan et al. (2012)
CF	Reductive dechlorination	biotic (*Dehalobacter* sp.UNSWDHB consortium)	laboratory	-4.3 ± 0.5	1	1	1	1.004	NM				NM	Lee et al. (2015)
CT	Reductive dechlorination	abiotic (goethite, magnetite, lepidocrocite, hematite, siderite)	laboratory	-26 to -32	1	1	1	1.027 to 1.033	NM				NM	Zwank et al. (2005); Elsner et al. (2004)
CT	Reductive dechlorination	abiotic (mackinawite)	laboratory	-10.9 to -15.9	1	1	1	1.011 to 1.016	NM				NM	Zwank et al. (2005); Neumann et al. (2009)
CT	Reductive dechlorination	abiotic (Zn(0))	laboratory	-10.8 ± 0.7	1	1	1	1.01	NM				NM	VanStone et al. (2008)
1,1,1-TCA	Reductive dechlorination	abiotic (Cr(II), Fe0 and Cu and Fe mixtures)	laboratory	-16 to -14	2	1	1	1.027 ± 0.002	NM				NM	Elsner et al. (2007)
1,1,1-TCA	Reductive dechlorination	abiotic (Fe(0))	laboratory	-7.8 ± 0.4	2	1	1	1.0158 ± 0.0008	-5.2 ±0.2	3	3	3	1.0160 ± 0.0006	1.5 ± 0.1	Palau et al. (2014a)
1,1,1-TCA	Reductive	abiotic (hydrolysis/	laboratory	-1.6 ± 0.2	2	1	1	1.0033 ±	-4.7 ±0.1	3	3	3	1.0145 ±	0.33	Palau et al. (2014a)

	dechlorination	dehydrohalogenation)						0.0004					0.0003	±0.04	
1,1,1-TCA	Reductive dechlorination	biotic	laboratory	-1.8 to -1.5	2	1	1	1.0036 ±0.0006	NM					NM	Sherwood Lollar et al. (2010)
1,2-DCA	Reductive dechlorination	abiotic (Zn(0))	laboratory	-29.7 ± 1.5	2	2	1	1.03	NM					NM	VanStone et al. (2008)
TCE	Reductive dechlorination	abiotic (Fe(0))	laboratory	-13 ± 2	2	1	1	1.0275	-2.6 ±0.1	3	1	1	1.008 ± 0.001	5.2 ±0.3	Audí-Miró et al. (2013)
TCE	Reductive dechlorination	abiotic (Fe(0))	field	-12	2	1	1	1.0254	-3.0	3	1	1	1.009	4.2	Lojkasek-Lima et al. (2012)
TCE	Reductive dechlorination	abiotic (FeS)	laboratory	-27.9 to -33.4	2	1	1	1.059 to 1.072	NM					NM	Liang et al. (2007)
TCE	Reductive dechlorination	abiotic (corrinoids)	laboratory	-15.0 to -18.5					-3.2 to -4.2					0.3 to 0.8	Renpenning et al. (2014)
TCE	Reductive dechlorination	abiotic (vitamin B12)	laboratory	-16.7 to -17.2	2	1	1	1.034 to 1.036							Slater et al. (2003)
TCE	Reductive dechlorination	abiotic (cyanocobalamin)	laboratory	-16.1 ±0.9	2	1	1	1.03	-4.0 ±0.2	3	1	1	1.01	3.9 ± 0.2	Cretnik et al. (2013)
TCE	Reductive dechlorination	biotic	laboratory	-8.8 ± 0.2	2	1	1	1.0179	-3.5 ± 0.5	3	1	1	1.0106	2.7 ± 0.1	Wiegert et al. (2013)
TCE	Reductive dechlorination	biotic (KB-1 consortium)	laboratory	-2.5 to -13.8	2	1	1	1.005 to 1.028	NM						Bloom et al. (2000): Slater et al. (2001)
TCE	Reductive dechlorination	biotic (*S. multivorans*, *D. michiganesis* BB1 and BD1 mixed *Dehaloc.* consortium)	laboratory	-4.1 to -15.3	2	1	1	1.008 to 1.0315	NM					NM	Liang et al. (2007)
TCE	Reductive dechlorination	biotic (*S. multivorans*)	laboratory	-20.0 to -20.2					-3.7 to -3.9					5.0 to -5.3	Renpenning et al. (2014)
TCE	Reductive dechlorination	biotic (*G. lovleyi* SZ, *D. hafniense* Y51)	laboratory	-9.1 to -12.2	2	1	1	1.02	-2.7 to -3.6	3	1	1	1.01	3.4 ± 0.2	Cretnik et al. (2013)
TCE	Reductive dechlorination	biotic (mixed *Dehaloc.* consortium)	laboratory	-16.4 ± 0.4	2	2	1	1.017 ± 0.000	-3.6 ± 0.3	3	3	1	1.004 ± 0.000	4.7	Kuder et al. (2013)
PCE	Reductive dechlorination	abiotic (corrinoids)	laboratory	-22.4 to -25.3					-3.4 to -4.8					4.6 to 7.0	Renpenning et al. (2014)
PCE	Reductive dechlorination	abiotic (vitamin B12)	laboratory	-15.8 to -16.5	2	2	2	1.033 to 1.034							Slater et al. (2003)
PCE	Reductive dechlorination	abiotic (FeS)	laboratory	-24.6 to -30.2	2	2	2	1.052 to 1.064	NM					NM	Liang et al. (2007)
PCE	Reductive dechlorination	biotic (*Desulfitobacterium*)	laboratory	-5.6 ± 0.7	2	2	2	1.0113	-2.0 ± 0.5	4	4	4	1.0081	2.5 ± 0.8	Wiegert et al. (2013)
PCE	Reductive dechlorination	biotic (*Desulfitobacterium* Viet1)	laboratory	-19.0 ±0.9	2	2	2	1.019	-5.0 ±0.1	4	4	4	1.005	3.8 ± 0.2	Cretnik et al. (2014)
PCE	Reductive dechlorination	biotic (*Sulfurospirillum*, PceATCE)	laboratory	-3.6 ± 0.2	2	2	2	1.007	-1.2 ± 0.1	4	4	4	1.005	2.7 ± 0.3	Badin et al. (2014)

PCE	Reductive dechlorination	biotic (*Sulfurospirillum*, PceADCE)	laboratory	-0.7 ± 0.1	2	2	2	1.001	-0.9 ±0.1	4	4	4	1.004	0.7 ± 0.2	Badin et al. (2014)
PCE	Reductive dechlorination	biotic (*S. multivorans*)	laboratory	-1.3 to -1.4					-0.4 to -0.6					2.2 to 2.8	Renpenning et al. (2014)
PCE	Reductive dechlorination	biotic (*S. multivorans*, *D. michiganesis* BB1 and BD1 mixed *Dehaloc.* consortium)	laboratory	-1.3 to -7.1	2	2	2	1.003 to 1.0415	NM					NM	Liang et al. (2007)
PCE	Reductive dechlorination	biotic	field	NA				NA	NA				NA	0.42 to 1.12	Wiegert et al. (2012)

[a] secondary isotope effect; NM: not measured; NA: not available; NAP: not applicable

References

Abe, Y.; Aravena, R.; Zopfi, J.; Shouakar-Stash, O.; Cox, E.; Roberts, J.D.; Hunkeler, D. Carbon and chlorine isotope fractionation during aerobic oxidation and reductive dechlorination of vinyl chloride and cis-1,2-dichloroethene. *Environ. Sci. Technol.* **2009**, 43, 101-107

Agrawal, A.; Tratnyek, P.G. Reduction of nitro aromatic compounds by zero-valent iron metal. *Environ. Sci. Technol.* **1996**, 30, 153-160

Arnold, W.A; Ball, W.P.; Roberts, A.L. Polychlorinated ethane reaction with zero-valent zinc: pathways and rate control. *J. Contam. Hydrol.* **1999**, 40, 183-200

Audí-Miró, C.; Cretnik, S.; Otero, N.; Palau, J.; Shouakar-Stash, O.; Soler, A.; Elsner, M. Cl and C isotope analysis to assess the effectiveness of chlorinated ethene degradation by zero-valent iron: Evidence from dual element and product isotope values. *Appl. Geochem.* **2013**, 32, 175-183

Badin, A.; Buttet, G.; Maillard, J.; Holliger, C.; Hunkeler, D. Multiple dual C–Cl isotope patterns associated with reductive dechlorination of tetrachloroethene. *Environ. Sci. Technol.* **2014**, 48, 9179-9186

Bastida, F.; Rosell, M.; Franchini, A. G.; Seifert, J.; Finsterbusch, S.; Jehmlich, N.; Jechalke, S.; von Bergen, M.; Richnow, H.H. Elucidating MTBE degradation in a mixed consortium using a multidisciplinary approach. *FEMS Microbiol. Ecol.* **2010**, 73, 370-384

Bernstein, A.; Shouakar-Stash, O.; Ebert, K.; Laskov, C.; Hunkeler, D.; Jeannottat, S.; Sakaguchi-Söder, K.; Laaks, J.; Jochmann, M.A.; Cretnik, S.; Jager, J.; Haderlein, S.B.; Schmidt, T.C.; Aravena, R.; Elsner, M. Compound-specific chlorine isotope analysis: A comparison of gas chromatography/isotope ratio mass spectrometry and gas chromatography/quadrupole mass spectrometry methods in an interlaboratory study. *Anal. Chem.* **2011**, 83, 7624-7634

Bloom, Y.; Aravena, R. ; Hunkeler, D. ; Edwards, E. ; Frape, S.K. Carbon isotope fractionation during microbial dechlorination of trichloroethene, cis-1,2-dichloroethene, and vinyl chloride: Implications for assessment of natural attenuation. *Environ. Sci. Technol.* **2000**, 34, 2768-2772

Borisov, Y.A.; Arcia, E.E.; Mielke, S.L.; Garrett, B.C.; Dunning, T.H. A systematic study of the reactions of OH- with chlorinated methanes. 1. Benchmark studies of the gas-phase reactions. *J. Phys. Chem. A* **2001**, 105, 7724-7736

Brunauer, S.; Emmet, P.H.; Teller, E. Adsorption of gases on multimolecular layers. *J. Am. Chem. Soc.* **1938**, 60, 309-319

Burris, D.R.; Campbell, T.J.; Manoranjan, V.S. Sorption of trichloroethylene and tetrachloroethylene in a batch reactive metallic iron-water system. *Environ. Sci. Technol.* **1995**, 29, 2850-2855

Burris, D.R.; Allen-King R.M.; Manoranjan, V.S.; Campbell, T.J.; Loraine, G.A.; Deng, B. Chlorinated ethane reduction by cast iron: Sorption and mass transfer. *J. Environm. Eng.-ASCE* **1998**, 124, 1012-1019

Chan, C.C.H.; Mundle, S.O.C.; Eckert, T.; Liang, X.; Tang, S.; Lacrampe-Couloume, G.; Edwards, E.A.; Sherwood Lollar, B. Large carbon isotope fractionation during biodegradation of chloroform by Dehalobacter cultures. *Environ. Sci. Technol.* **2012**, 46, 10154-10160

Choe, S.; Lee, S.H.; Chang, Y.Y.; Hwang, K.Y.; Khim, J. Rapid reductive destruction of hazardous organic compounds by nanoscale Fe-0. *Chemosphere* **2001**, 42, 367-372.

Coplen, T.B.; Brand, W.A.; Gehre, M.; Gröning, M.; Meijer, H.A.J.; Toman, B.; Verkouteren, R.M. After two decades a second anchor for the VPDB $\delta^{13}C$ scale. *Rapid Commun. Mass Spectrom.* **2006**, 20, 3165-3166

Cretnik, S.; Thoreson, K.A.; Bernstein, A.; Ebert, K.; Buchner, D.; Laskov, C.; Haderlein, S.; Shouakar-Stash, O.; Kliegman, S.; McNeill, K.; Elsner, M. Reductive dechlorination of TCE by chemical model systems in comparison to dehalogenating bacteria: Insights from dual element isotope analysis ($^{13}C/^{12}C$, $^{37}Cl/^{35}Cl$). *Environ. Sci. Technol.* **2013**, 47, 6855-6863

Cretnik, S.; Bernstein, A.; Shouakar-Stash, O.; Löffler, F.; Elsner, M. Chlorine isotope effects from isotope ratio mass spectrometry suggest intramolecular C-Cl bond competition in trichloroethene (TCE) reductive dehalogenation. *Molecules* **2014**, 19, 6450-6473

Dayan, H.; Abrajano, T.; Sturchio, N.C.; Winsor, L. Carbon isotopic fractionation during reductive dehalogenation of chlorinated ethenes by metallic iron. *Org. Geochem.* **1999**, 30, 755-763

Dorer, C.; Vogt, C.; Neu, T.R.; Kleinsteuber, S.; Stryhanyuk, H.; Richnow, H.-H. Characterization of toluene and ethylbenzene biodegradation under nitrate-, iron(III)- and manganese(IV)-reducing conditions by compound-specific isotope analysis. *Environ. Pollut.* **2016**, 211, 271-281

Dybala-Defratyka, A.; Rostkowski, M.; Matsson, O.; Westaway, K.C.; Paneth, P. A new interpretation of chlorine leaving group kinetic isotope effects; A theoretical approach. *J. Org. Chem.* **2004**, 69, 4900-4905

Elsner, M.; Chartrand, M.; VanStone, N.; Lacrampe-Couloume, G.; Sherwood Lollar, B. Identifying abiotic chlorinated ethene degradation: Characteristic isotope patterns in reaction products with nanoscale zero-valent iron. *Environ. Sci. Technol.* **2008**, 42, 5963-5970

Elsner, M.; Cwiertny, D.M.; Roberts, A.L.; Sherwood Lollar, B. 1,1,2,2-tetrachloroethane reactions with OH^-, Cr(II), granular iron, and a copper-iron bimetal: Insights from product formation and associated carbon isotope fractionation. *Environ. Sci. Technol.* **2007**, 41, 4111-4117

Elsner, M.; Haderlein, S.B.; Kellerhals, T.; Luzi, S.; Zwank, L.; Angst, W.; Schwarzenbach, R.P. Mechanisms and products of surface-mediated reductive dehalogenation of carbon tetrachloride by Fe(II) on goethite. *Environ. Sci. Technol.* **2004**, 38, 2058-2066

Elsner, M.; Hunkeler, D. Evaluating chlorine isotope effects from isotope ratios and mass spectra of polychlorinated molecules. *Anal. Chem.* **2008**, 80, 4731-4740

Elsner, M.; Zwank, L.; Hunkeler, D.; Schwarzenbach, R.P. A new concept linking observable stable isotope fractionation to transformation pathways of organic pollutants. *Environ. Sci. Technol.* **2005**, 39, 6896-6916

Feng, J.; Lim, T.-T. Pathways and kinetics of carbon tetrachloride and chloroform reductions by nano-scale Fe and Fe/Ni particles: comparison with commercial micro-scale Fe and Zn. *Chemosphere* **2005**, 59, 1267-1277

Gray, J.R.; Lacrampe-Couloume, G.; Gandhi, D.; Scow, K.M.; Wilson, R.D.; Mackay, D.M.; Sherwood Lollar, B. Carbon and hydrogen isotopic fractionation during biodegradation of methyl tertbutyl ether. *Environ. Sci. Technol.* **2002**, 36, 1931-1938

Hardy, L.I.; Gillham, R.W. Formation of hydrocarbons from the reduction of aqueous CO_2 by zero-valent iron. *Environ. Sci. Technol*. **1996**, 30, 57-65

Heckel, B.; Rodríguez-Fernández, D.; Torrentó, D.; Meyer, A.; Palau, J.; Domènech, C.; Rosell, M.; Soler, A.; Hunkeler, D.; Elsner, D. Compound-specific chlorine isotope analysis of tetrachloro-methane and trichloromethane by GC-IRMS vs. GC-qMS: Method development and evaluation of precision and trueness. *Anal. Chem.* **2017**, 89, 3411-3420

Heraty, L.J.; Fuller, M.E.; Huang, L.; Abrajano, T.; Sturchio, N. C. Isotope fractionation of carbon and chlorine by microbial degradation of dichloromethane. *Org. Geochem.* **1999**, 30, 793-799

Herrmann, S.; Vogt, C.; Fischer, A.; Kuppardt, A.; Richnow, H.-H. Characterization of anaerobic xylene biodegradation by two-dimensional isotope fractionation analysis. *Environ. Microbiol. Rep.* **2009**, 1, 535-544

Hine, J. Carbon dichloride as an intermediate in the basic hydrolysis of chloroform. A mechanism for substitution reactions at a saturated carbon atom. *J. Am. Chem. Soc.* **1950**, 72, 2438-2445

Hirschorn, S.K.; Dinglasan, M.J.; Elsner, M.; Mancini, S.A.; Lacrampe-Couloume, G. ; Edwards,‖E.A.; Sherwood Lollar, B. Pathway dependent isotopic fractionation during aerobic biodegradation of 1,2-dichloroethane. *Environ. Sci. Technol.* **2004**, 38, 4775-4781

Hofstetter, T.B.; Spain, J.C.; Nishino, S.F.; Bolotin, J.; Schwarzenbach, R.P. Identifying competing aerobic nitrobenzene biodegradation pathways using compound-specific isotope analysis. *Environ. Sci. Technol.* **2008**, 42, 4764-4770

Holt, B.D.; Sturchio, N.C.; Abrajano, T.A.; Heraty, L.J. Conversion of chlorinated volatile organic compounds to carbon dioxide and methyl chloride for isotopic analysis of carbon and chlorine. *Anal. Chem.* **1997**, 69, 2727-2733

Huang, K.C.; Zhao, Z.; Hoag, G.E.; Dahmani, A.; Block, P.A. Degradation of volatile organic compounds with thermally activated persulfate oxidation. *Chemosphere* **2005**, 61, 551-560

Hunkeler, D.; Butler, B.J.; Aravena, R.; Barker, J.F. Monitoring biodegradation of methyl tert-butyl ether (MTBE) using compoundspecific carbon isotope analysis. *Environ. Sci. Technol.* **2001**, 35, 676-681

Johnson, T.L.; Scherer, M.M.; Tratnyek, P.G. Kinetics of halogenated organic compound reduction by iron metal. *Environ. Sci. Technol.* **1996**, 2634-2640

Jung, J.-G.; Do, S.-H.; Kwon, Y.-J.; Kong, S.-H. Degradation of multi-DNAPLs by a UV/persulphate/ethanol system with the additional injection of a base solution. *Environ. Technol.* **2015**, 36, 1044-1049

Kowalski, K.; Valiev, M. Extensive regularization of the coupled cluster methods based on the generating functional formalism: Application to gas-phase benchmarks and to the S_N2 reaction of $CHCl_3$ and OH^- in water. *J. Chem. Phys.* **2009**, 131, 234107

Kozell, A.; Yecheskel, Y.; Balaban, N.; Dror, I.; Halicz, L.; Ronen, Z.; Gelman, F. Application of dual carbon−bromine isotope analysis for investigating abiotic transformations of tribromoneopentyl alcohol (TBNPA). *Environ. Sci. Technol.* **2015**, 49, 4433-4440

Kuder, T.; van Breukelen, B.M.; Vanderford, M.; Philp, P. 3D-CSIA: Carbon, chlorine, and hydrogen isotope fractionation in transformation of TCE to ethene by a *Dehalococcoides* culture. *Environ. Sci. Technol.* **2013**, 47, 9668-9677

Lee, M.; Wells, E.; Wong, Y.K.; Koenig, J.; Adrian, L.; Richnow, H.H.; Manefield, M. Relative contributions of *Dehalobacter* and zerovalent iron in the degradation of chlorinated methanes. *Environ. Sci. Technol.* **2015**, 49, 4481-4489

Li, T.; Farrell, J. Reductive dechlorination of trichloroethene and carbon tetrachloride using iron and palladized-iron cathodes. *Environ. Sci. Technol.* **2000**, 34, 173-179

Liang, X.; Dong, Y.; Kuder, T.; Krumholz, L.R.; Philp, R.P.; Butler, E.C. Distinguishing abiotic and biotic transformation of tetrachloroethylene and trichloroethylene by stable carbon isotope fractionation. *Environ. Sci. Technol.* **2007**, 41, 7094-7100

Lien, H.-L.; Zhang, W.-X. Transformation of chlorinated methanes by nanoscale iron particles. J. *Environ. Eng.* **1999**, 125, 1042-1047

Lojkasek-Lima, P.; Aravena, R.; Shouakar-Stash, O.; Frape, S.K.; Marchesi, M.; Fiorenza, S.; Vogan, J. Evaluating TCE abiotic and biotic degradation pathways in a permeable reactive barrier using compound specific isotope analysis. *Ground Water Monit. Remediat.* **2012**, 32, 53-62

Matheson, L.J.; Tratnyek, P.G. Reductive dehalogenation of chlorinated methanes by iron metal. *Environ. Sci. Technol.* **1994**, 2045-2053

Meckenstock, R.U.; Morasch, B.; Warthmann, R.; Schink, B.; Annweiler, E.; Michaelis, W.; Richnow, H.H. C-13/C-12 isotope fractionation of aromatic hydrocarbons during microbial degradation. *Environ Microbiol.* **1999**, 1, 409-414

Merrigan, S.R.; Le Gloahec, V.N.; Smith, J.A.; Barton, D.H.R.; Singleton, D.A. Separation of the primary and secondary kinetic isotope effects at a reactive center using starting material reactivities. Application to the $FeCl_3$-catalyzed oxidation of C-H bonds with tertbutyl hydroperoxide. *Tetrahedron Lett.* **1999**, 40, 3847-3850

Meyer, A.H.; Dybala-Defratyka, A.; Alaimo, P.J.; Geronimo, I.; Sanchez, A.D.; Cramer, C.J.; Elsner, M. Cytochrome P450-catalyzed dealklyation of atrazine by *Rhodococcus* sp. strain NI86/21 involves hydrogen atom transfer rather than single electron transfer. *Dalton Trans.* **2014**, 43, 12111-12432

Miller, L.G.; Kalin, R.M.; McCauley, S.E.; Hamilton, J.T.G.; Harper, D.B.; Millet, D.B.; Oremland, R.S.; Goldstein, A.H. Large carbon isotope fractionation associated with oxidation of methyl halides by methylotrophic bacteria. *Proc. Natl. Acad.Sci. U.S.A.* **2001**, 98, 5833-5837

Neumann, A.; Hofstetter, T.B.; Skarpeli-Liati, M.; Schwarzenbach, R.P. Reduction of polychlorinated ethanes and carbon tetrachloride by structural Fe(II) in smectites. *Environ. Sci. Technol.* **2009**, 43, 4082-4089

Nurmi, J.T.; Tratnyek, P.G.; Sarathy, V.; Amonette, J.E.; Pecher, K.; Wang, C.; Linehan, J.C.; Matson, D.W.; Penn, R.L.; Driessen, M.D. Characterization and properties of metallic iron nanosized particles: Spectroscopy, electrochemistry, and kinetics. *Environ. Sci. Technol.* **2005**, 39, 1221-1230

Palau, J.; Soler, A.; Teixidor, P.; Aravena, R. Compound-specific carbon isotope analysis of volatile organic compounds in water using solid-phase microextraction. *J. Chromatogr.* A **2007**, 1163, 260-268

Palau, J.; Shouakar-Stash, O.; Hunkeler, D. Carbon and chlorine isotope analysis to identify abiotic degradation pathways of 1,1,1-trichloroethane. *Environ. Sci. Technol.* **2014a**, 48, 14400-14408

Palau, J; Cretnik, S.; Shouakar-Stash, O.; Höche, M.; Elsner, M.; Hunkeler, M. C and Cl isotope fractionation of 1,2-dichloroethane displays unique $\delta^{13}C/\delta^{37}Cl$ patterns for pathway identification and reveals surprising C−Cl bond involvement in microbial oxidation. *Environ. Sci. Technol.* **2014b**, 48, 9430-9437

Pati, S.G.; Kohler, H.-P.E.; Bolotin, J.; Parales, R.E.; Hofstetter, T.B. Isotope effects of enzymatic dioxygenation of nitrobenzene and 2−nitrotoluene by nitrobenzene dioxygenase. *Environ. Sci. Technol.* **2014**, 48, 10750-10759

Penning, H.; Sorensen, S.R.; Meyer, A.H.; Aamand, J.; Elsner, M. C, N, and H isotope fractionation of the herbicide isoproturon reflects different microbial transformation pathways. *Environ. Sci. Technol*. **2010**, 44, 2372-2378

Pohl, L.R.; Bhooshan, B.; Whittaker, N.F.; Krishna, G. Phosgene: a metabolite of chloroform. *Biochem. Bioph. Res. Co.* **1977**, 79, 684-691

Renpenning, J.; Keller, S.; Cretnik, S.; Shouakar-Stash, O.; Elsner, M.; Schubert, T.; Nijenhuis, I. Combined C and Cl isotope effects indicate differences between corrinoids and enzyme

(*Sulfurospirillum multivorans* PceA) in reductive dehalogenation of tetrachloroethene, but not trichloroethene. *Environ. Sci. Technol.* **2014**, 48, 11837-11845

Roberts, P.V.; Cornel, P.; Summers, R.S. External mass-transfer rate in fixed-bed adsorption. *J. Environ. Eng.* **1985**, 111, 891-905

Rosell, M.; Barcelo, D.; Rohwerder, T.; Breuer, U.; Gehre, M.; Richnow, H.H. Variations in $^{13}C/^{12}C$ and D/H enrichment factors of aerobic bacterial fuel oxygenate degradation. *Environ. Sci. Technol.* **2007**, 41, 2036-2043

Rosell, M.; Finsterbusch, S.; Jechalke, S.; Hübschmann, T.; Vogt, C.; Richnow, H.H. Evaluation of the effects of low oxygen concentration on stable isotope fractionation during aerobic MTBE biodegradation. *Environ. Sci. Technol.* **2010**, 44, 309-315

Sherwood Lollar, B.; Hirschorn, S.; Mundle, S.O.C.; Grostern, A.; Edwards, E.A.; Lacrampe-Couloume, G. Insights into enzyme kinetics of chloroethane biodegradation using compound specific stable isotopes. *Environ. Sci. Technol.* **2010**, 44, 7498-7503

Skell, P.S.; Hauser, C.R. The mechanism of beta-elimination with alkyl halides. *J. Am. Chem. Soc.* **1945**, 67, 1661-1661

Slater, G.F.; Sherwood Lollar, B.; Sleep, B.E.; Edwards, A.E. Variability in carbon isotopic fractionation during biodegradation of chlorinated ethenes: Implications for field applications. *Environ. Sci. Technol.* **2001**, 35, 901-907

Slater, G.F.; Sherwood Lollar, B.; King, A.; O'Hannesin, S. Isotopic fractionation during reductive dechlorination of trichloroethene by zero-valent iron: influence of surface treatment. *Chemosphere* **2002**, 49, 587-596

Slater, G.F.; Sherwood Lollar, B.; Lesage, S.; Brown, S. Carbon isotope fractionation of PCE and TCE during dechlorination by vitamin B12. *Ground Water Monit. Remediat.* **2003**, 23, 59-67

Song, H.H.; Carraway, E.R. Reduction of chlorinated methanes by nano-sized zero-valent iron. Kinetics, pathways, and effect of reaction conditions. *Environ. Eng. Sci.* **2006**, 23, 272-284

Támara, M.; Butler, E.C. Effects of iron purity and groundwater characteristics on rates and products in the degradation of carbon tetrachloride by iron metal. *Environ. Sci. Technol.* **2004**, 38, 1866-1876

Torrentó, C.; Audí-Miró, C.; Bordeleau, G.; Marchesi, M.; Rosell, M.; Otero, N.; Soler, A. The use of alkaline hydrolysis as a novel strategy for chloroform remediation: feasibility of using urban construction wastes and evaluation of carbon isotopic fractionation. *Environ. Sci. Technol.* **2014**, 48, 1869-1877

Valiev, M.; Garrett, B.C.; Tsai, M.-K.; Kowalski, K.; Kathmann, S.M.; Schenter, G.K.; Dupuis, M. Hybrid approach for free energy calculations with high-level methods: Application to the S_N2 reaction of $CHCl_3$ and OH^- in water. *J. Chem. Phys.* **2007**, 127, 051102-1-4

VanStone, N.; Elsner, M.; Lacrampe-Couloume, G.; Mabury, S.; Sherwood Lollar, B. Potential for identifying abiotic chloroalkane degradation mechanisms using carbon isotopic fractionation. *Environ. Sci. Technol.* **2008**, 42, 126-132

Vogt, C.; Cyrus, E.; Herklotz, I.; Schlosser, D.; Bahr, A.; Herrmann, S.; Richnow, H.-H.; Fischer, A. Evaluation of toluene degradation pathways by two-dimensional stable isotope fractionation. *Environ. Sci. Technol.* **2008**, 42, 7793-7800

Wiegert, C.; Aeppli, C.; Knowles, T.; Holmstrand, H.; Evershed, R.; Pancost, R.D. ; Macháčková, J.; Gustafsson, O. Dual carbon-chlorine stable isotope investigation of sources and fate of chlorinated ethenes in contaminated groundwater. *Environ. Sci. Technol.* **2012**, 46, 10918-10925

Wiegert, C.; Mandalakis, M.; Knowles, T.; Polymenakou, P.; Aeppli, C.; Machackova, J.; Holmstrand, H.; Evershed, R.P.; Pancost, R.; Gustafsson, O. Carbon and chlorine isotope fractionation during microbial degradation of tetra- and trichloroethene. *Environ. Sci. Technol.* **2013**, 47, 6449-6456

Zhu, X.; Du, E.; Ding, H.; Lin, Y.; Long, T.; Li, H.; Wang, L. QSAR modeling of VOCs degradation by ferrous-activated persulfate oxidation. *Desalin. Water Treat.* **2015**, 1-15

Zwank, L.; Elsner, M.; Aeberhard, A.; Schwarzenbach, R.P. Carbon isotope fractionation in the reductive dehalogenation of carbon tetrachloride at iron (hydr)oxide and irons minerals. *Environ. Sci. Technol.* **2005**, 39, 5634-5641